J|A|C|S
COMMUNICATIONS

Published on Web 02/21/2006

Facile Autoreduction of Iron Oxide/Carbon Nanotube Encapsulates

Wei Chen,[†] Xiulian Pan,[†] Marc-Georg Willinger,[‡] Dang Sheng Su,[‡] and Xinhe Bao*[,†]

State Key Laboratory of Catalysis, Dalian Institute of Chemical Physics, The Chinese Academy of Sciences, Dalian 116023, P. R. China, and Department of Inorganic Chemistry, Fritz Haber Institute of the Max Planck Society, Berlin D-14195, Germany

Received September 30, 2005; E-mail: xhbao@dicp.ac.cn

Carbon nanotubes (CNTs) have been proposed as nanoreactors, due to the well-defined structure in terms of inner hollow cavities and a high aspect ratio.[1] Several successful applications were reported, including synthesis of nanostructured materials under mild conditions (e.g., SiC,[2] β-zeolite,[3] and $CoFe_2O_4$ nanowires[3]). Some chemical reactions confined within these nanochannels were also found to exhibit higher activities.[3,4] We are interested in CNT-confined iron since iron is an important transition metal and is widely used as a catalyst for Fisher Tropsch and ammonia synthesis.[5,6] However, the confinement of elemental transition metals in CNTs is still a challenge. Most often, metal/CNT encapsulates are obtained by adsorption of precursors with subsequent reduction in H_2-containing streams[7] or direct incorporation during pyrolysis of precursor mixtures, such as ferrocene−acetylene.[8] In this paper, we present direct experimental evidence of facile reduction of Fe_2O_3 nanoparticles located inside the bores (inner particles) at 600 °C versus reduction of those on the outer surface of multi-walled CNTs (outer particles) at 800 °C. To the best of our knowledge, this is the first example of CNT-confined particles of d-band metals obtained through direct reduction of incorporated oxide nanoparticles by the CNT host.

Multi-walled CNTs with 4−8 nm i.d. and 10−20 nm o.d. (Chengdu Organic Chemicals Co., LTD) were loaded with Fe_2O_3 (8 wt %) (Supporting Information, SI-1 and -2). The changes of Fe_2O_3 particles with the temperature were monitored in situ by HRTEM (Philips CM200 FEG) during heating to 600 °C. To avoid the influence of long time exposure to the electron beam, we have imaged many particles randomly before and after heating (SI-3). Figure 1 displays HRTEM images of Fe_2O_3/o-CNTs with Fe_2O_3 particles deposited on CNTs with opened tips (SI-1 and -2). We observed that Fe_2O_3 particles have a uniform size around 5−7 nm with 80 ± 10% of the particles located in the bores and the rest on the outer surface. The Fast Fourier Transforms shown in the insets of Figure 1 reveal a typical CNT *d* spacing of 3.50 ± 0.05 Å in the whole temperature range. At 20 °C, Fe_2O_3 particles with 2.47 ± 0.05 and 2.80 ± 0.05 Å *d* spacings corresponding to the [311] and [300] planes of Fe_2O_3, respectively, were observed both inside and outside the nanotubes (Figures 1 and SI-3). In situ TEM revealed that up to 600 °C the 2.47 and 2.80 Å *d* spacings of outer particles remained unchanged (Figures 1 and SI-3). However, the *d* spacing of inner particles changed to 1.98 ± 0.05 Å at 600 °C, characteristic of Fe [110], which indicates the reduction of Fe_2O_3 to Fe.

$$Fe_2O_3(\text{inner})/\text{o-CNTs} \xrightarrow{600\ ^\circ C} Fe(\text{inner})/\text{o-CNTs} + CO$$

Additional XRD was carried out by heating samples ex situ in a He stream (SI-4). Figure 2a exhibits four broad peaks, typical of

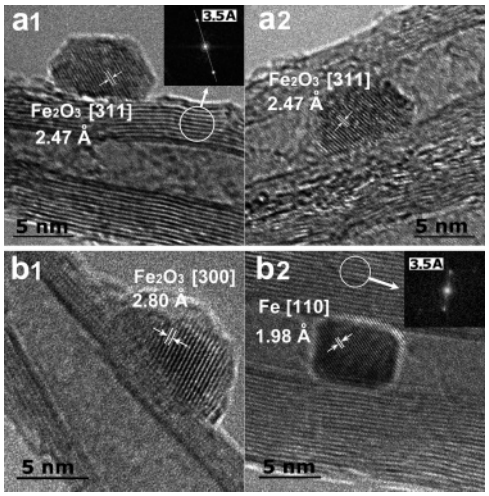

Figure 1. In situ HRTEM images of Fe_2O_3/o-CNTs at (a) 20 °C and (b) 600 °C. (a1) and (b1) show outer particles, (a2) and (b2) inner particles with typical crystal planes. The insets in (a1) and (b2) show the Fast Fourier Transform diffraction of CNTs at corresponding temperatures.

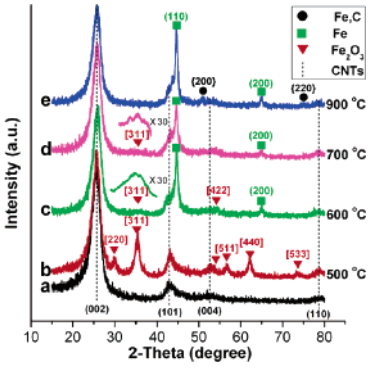

Figure 2. XRD patterns of (a) o-CNTs and Fe_2O_3/o-CNTs heated to (b) 500 °C, (c) 600 °C, (d) 700 °C, and (e) 900 °C.

CNTs. In addition, diffraction lines corresponding to Fe_2O_3 [220], [311], [511], [440], and [533] (JCPDS 04-0755) (marked with triangles) are detected in Fe_2O_3/o-CNTs between 20 and 500 °C (Figure 2b). Figure 2c demonstrates that a transformation has taken place in Fe_2O_3/o-CNTs at 600 °C. New peaks (marked with squares) can be indexed to Fe [110] and [200] (JCPDS 06-0696), respectively, while the diffraction peaks of Fe_2O_3 have disappeared except for very weak Fe_2O_3 [311] and [422] signals (triangles). The Fe_2O_3 [311] peak is still observable at 700 °C, while it has disappeared completely at 900 °C (Figure 2d,e). The weak Fe_2O_3 peaks above 600 °C may be due to the small amount of the outer particles. These ex situ XRD results corroborate the in situ HRTEM observation of the reduction of the inner Fe_2O_3 particles around 600 °C, while the outer ones remain oxide.

[†] Dalian Institute of Chemical Physics.
[‡] Fritz Haber Institute of the Max Planck Society.

10.1021/ja056721l CCC: $33.50

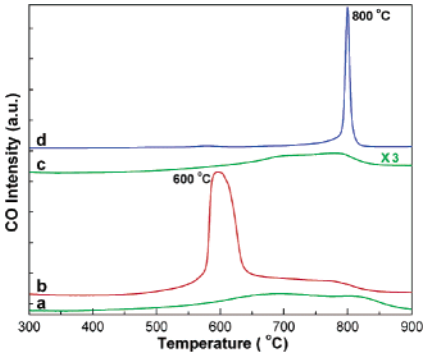

Figure 3. Temperature-programmed desorption of CO: (a) o-CNTs; (b) Fe_2O_3/o-CNTs; (c) c-CNTs; (d) Fe_2O_3/c-CNTs.

Temperature-programmed desorption (TPD) was carried out in a He stream, and the effluents were monitored by an on-line mass spectrometer (SI-5). Significant desorption of CO_2 was only observed below 600 °C, and it was very similar for both o-CNTs and Fe_2O_3/o-CNTs (Figure SI-6). Figure 3a shows two broad CO desorption peaks of o-CNTs between 450 and 900 °C, which arise from the decomposition of carbonyl, ether, and other surface oxygen groups (SOGs).[9] An additional intense CO desorption peak was observed around 600 °C from Fe_2O_3/o-CNTs (Figure 3b). This is attributed to the reduction of the inner Fe_2O_3 particles, in agreement with the appearance of metallic iron at this temperature detected by XRD and TEM. To confirm the higher reduction temperature of outer particles, we also deposited Fe_2O_3 on the outer surface of CNTs with closed tips, c-CNTs (SI-1 and -2).

c-CNTs yielded CO TPD profiles similar to those of o-CNTs (Figure 3c), but with a much lower intensity (the intensity of Figure 3c has been scaled up by a factor of 3). This indicates that there are similar but fewer SOGs on the surface of c-CNTs compared to o-CNTs. Therefore, the nature of the interaction between SOGs and outer particles in Fe_2O_3/c-CNTs and Fe_2O_3/o-CNTs should be comparable. The TPD profile of Fe_2O_3/c-CNTs (Figure 3d) does not show the intense peak at 600 °C but a sharp peak around 800 °C, in addition to the broad bands due to SOGs, indicating a quick reduction of homogeneous Fe_2O_3 particles. This much higher reduction temperature for the outer particles in Fe_2O_3/c-CNTs is consistent with the XRD and TEM results of Fe_2O_3/o-CNTs. We also found that the reduction of Fe_2O_3 deposited on activated carbon (AC) (Vulcan XC-72, Cabot Corp.) takes place around 723 °C (SI-7), lying between the one for the inner and outer particles deposited on CNTs. Prabhakaran et al. further reported that the reduction of Fe_2O_3 particles supported on a graphite surface was not observed using XPS even after annealing at 800 °C in UHV.[10]

From the above data, one clearly sees the facile reduction of Fe_2O_3 located in the CNT bores. SOGs may contribute to the reduction of Fe_2O_3. However, the interaction of Fe_2O_3 with similar, but less abundant, SOGs in Fe_2O_3/c-CNTs should change the intensity but not the temperature of CO evolution compared to Fe_2O_3/o-CNTs. SOGs could also affect the electron structure of the CNTs.[11] However, this should be the same for SOGs located on the inner and outer CNT surfaces, and thus a pronounced difference in the reduction temperature for inner and outer particles would not be expected.

On the other hand, Haddon used π-orbital axis vector analysis to show that the chemistry of fullerene-type carbon relates directly to the strain of the graphitic network.[12] Deviation from planarity causes the partial rehybridization from sp^2 to sp^3 and the pyramidalization of the carbon atoms in curved aromatic systems.[12−15] As a result, π-electron density is shifted from the concave inner to the convex outer surface, and this shift is enhanced as the CNT cross-section becomes smaller.[12,14,15] Therefore, the interaction between the electron-deficient concave surface of the nanotube and the anionic oxygen in Fe_2O_3 could lead to weakened bonding strength of Fe_2O_3 and hence lower the activation energy for the reduction in the bores. Thus, Fe could form at the very low temperature of 600 °C. In contrast, for the outer particles, the interaction of the oxygen in Fe_2O_3 with the electron density-enriched outer nanotube surface should be weakened and/or become similar to that with graphite. Therefore, a higher temperature than that for the reaction with the inner CNT surface or AC is needed to initiate the reduction as observed. Thus, this mechanism can account readily for the observed differences in the reduction of the inner and outer Fe_2O_3 particles in CNTs.

In summary, the formation of metallic Fe is observed in the o-CNT bores at the low temperature of 600 °C relative to the reduction of Fe_2O_3 at 800 °C on the outer surface of c-CNTs. This is the first example of CNT-confined metal particles obtained by direct reduction by CNTs, which proves that nanotubes provide a confined environment with unique electronic properties. Further experiments and theoretical calculations are underway to elucidate the curvature-induced effects on the facilitated reduction of Fe_2O_3, as well as other transition metal oxides. These findings are relevant for analogous systems with encapsulated species and provide a base for development of new functional materials and/or catalysts with unique properties.

Acknowledgment. We thank Mr. X. Wei for the help on the XRD measurements, and Dr. A. Goldbach for fruitful discussions. The work was supported by a grant from the National Natural Science Foundation of China (Project No. 20503033).

Supporting Information Available: Preparation procedures of o-CNTs, c-CNTs, deposition of Fe_2O_3, and descriptions of TEM, XRD, and TPD experiments. This material is available free of charge via the Internet at http://pubs.acs.org.

References

(1) Dujardin, E.; Ebbesen, T. W.; Hiura, H.; Tanigaki, K. *Science* **1994**, *265*, 1850.
(2) Sun, X. H.; Li, C. P.; Wong, W. K.; Wong, N. B.; Lee, C. S.; Lee, S. T.; Teo, B. K. *J. Am. Chem. Soc.* **2002**, *124*, 14464.
(3) Nhut, J. M.; Pesant, L.; Tessonnier, J. P.; Winé, G.; Guille, J.; Pham-Huu, C.; Ledoux, M. J. *Appl. Catal. A* **2003**, *254*, 345.
(4) Zhang, Y.; Zhang, H. B.; Lin, G. D.; Chen, P.; Yuan, Y. Z.; Tsai K. R. *Appl. Catal. A* **1999**, *187*, 213.
(5) Menon, M.; Andriotis, A. N.; Froudakis, G. E. *Chem. Phys. Lett.* **2000**, *320*, 425.
(6) Westerberg, S.; Wang, C.; Chou, K.; Somorjai, G. A. *J. Phys. Chem. B* **2004**, *108*, 6374.
(7) Chen, Y. K.; Chu, A.; Cook, J.; Green, M. L. H.; Harris, P. J. F.; Heesom, R.; Humphries, M.; Sloan, J.; Tsang, S. C.; Turner, J. F. C. *J. Mater. Chem.* **1997**, *7*, 545.
(8) Karmakar, S.; Sharma, S. M.; Teredesai, P. V.; Sood, A. K. *Phys. Rev. B* **2004**, *69*, 165414.
(9) Boehm, H. P. *Carbon* **2002**, *40*, 145.
(10) Prabhakaran, K.; Shafi, K. V. P. M.; Ulman, A.; Ajayan, P. M.; Homma, Y.; Ogino, T. *Surf. Sci.* **2002**, *506*, L250.
(11) Hirsch, A. *Angew. Chem., Int. Ed.* **2002**, *41*, 1853.
(12) Haddon, R. C. *Science* **1993**, *261*, 1545.
(13) Dai, H. J. *Acc. Chem. Res.* **2002**, *35*, 1035.
(14) Menke, K.; Hopf, H. *Angew. Chem., Int. Ed. Engl.* **1976**, *15*, 165.
(15) Ugarte, D.; Chatelain, A.; de Heer, W. A. *Science* **1996**, *274*, 1897.

JA056721L